Tree Physiology 40, 841–855
doi:10.1093/treephys/tpaa028

Research paper

Freezing stress survival mechanisms in *Vaccinium macrocarpon* Ait. terminal buds

Camilo Villouta[1], Beth Ann Workmaster[1], Jenny Bolivar-Medina[2], Smith Sinclair[1] and Amaya Atucha[1,3]

[1]Department of Horticulture, University of Wisconsin-Madison, 1575 Linden Drive, Madison, WI 53706, USA; [2]Tree Fruit Research and Extension Center, Washington State University, 1100 N Western Ave, Wenatchee, WA 98801, USA; [3]Corresponding author (atucha@wisc.edu)

Received November 18, 2019; accepted February 20, 2020; handling Editor: Hisayo Yamane

Plants' mechanisms for surviving freezing stresses are essential adaptations that allow their existence in environments with extreme winter temperatures. Although it is known that *Vaccinium macrocarpon* Ait. buds can acclimate in fall and survive very cold temperatures during the winter, the mechanism for survival of these buds is not known. The main objective of this study was to determine which of the two major mechanisms of freezing stress survival, namely, deep supercooling or freeze-induced dehydration, are employed by *V. macrocarpon* terminal buds. In the present study, no low-temperature exotherms (LTEs) were detected by differential thermal analysis. Furthermore, a gradual reduction of relative liquid water content in the inner portions of buds during magnetic resonance imaging (MRI) scans performed between 0 and −20 °C (where no damage was detected in controlled freezing tests (CFT)) indicates these buds may not deep supercool. The higher ice nucleation activity of outer bud scales and the appearance of large voids in this structure in early winter, in conjunction with the MRI observations, are evidence supportive of a freeze-induced dehydration process. In addition, the presence of tissue browning in acclimated buds as a result of freezing stress was only observed in CFT at temperatures below −20 °C, and this damage gradually increased as test temperatures decreased and at different rates depending on the bud structure. Ours is the first study to collect multiple lines of evidence to suggest that *V. macrocarpon* terminal buds survive long periods of freezing stress by freeze-induced dehydration. Our results provide a framework for future studies of cold hardiness dynamics for *V. macrocarpon* and other woody perennial species and for the screening of breeding populations for freezing stress tolerance traits.

Keywords: cold hardiness, controlled freezing test, differential thermal analysis, freeze-induced dehydration, ice nucleation activity, MRI.

Introduction

Bud freezing stress survival is one of the main factors determining woody plant geographical distribution and is also a key antidote to the threat of economic losses in cultivated crops (George et al. 1974*a*, 1982, Levitt 1980, Snyder and de Melo-Abreu 2005). The risks from current and impending climate change include increased frequency and duration of extreme weather events (Vasseur et al. 2014, Williams et al. 2015), which will result in plants being increasingly more susceptible to damage by freezing stress (Gu et al. 2008). Greater understanding of the specific mechanisms by which plant tissue, such as woody plant buds, survive freezing stress is key to the identification of the physiological basis of genotypic variation in freezing tolerance. This will provide tools for the development of plant materials with enhanced freezing tolerance, in addition to improved plant management and agricultural decision-making.

The inner bud tissues of different woody plant species are known to survive freezing stress by alternative strategies: deep supercooling (freezing avoidance) and freeze-induced dehydra-

tion (tolerance) (Sakai 1982). While the two strategies share the common mechanism of bud scales tolerating the presence of extracellular ice formation, the mechanisms by which the inner bud tissues survives differ (Pearce 2001, Wisniewski et al. 2014). In deep supercooling, physical or structural modifications prevent the nucleation of ice in florets and meristems by keeping small amounts of water sequestered (Quamme 1974, Andrews and Proebsting 1986), even to extreme subfreezing temperatures. These tissues do not dehydrate (Quamme 1978, Quamme et al. 1995) or only do so very slowly, as significant minimum winter temperatures are reached (Wisniewski 1995, Wisniewski et al. 2014). When the critical nucleating temperatures for this sequestered water are reached, ice propagation is rapid, and the cellular damage is lethal (Quamme et al. 1995). Several studies have documented this phenomenon by measuring the exotherm released from the heat of fusion by utilizing differential thermal analysis (DTA) and other methods of temperature monitoring (George et al. 1974*b*, Quamme 1978, Andrews and Proebsting 1986, Kang et al. 1998, Mills et al. 2006). In contrast, freeze-induced dehydration involves the gradual loss of liquid water from the inner bud tissues, a process driven by the vapor pressure deficit established by the extracellular ice in bud scales (Sakai 1979, Ishikawa and Sakai 1981, 1985, Ishikawa 1982, Flinn and Ashworth 1994*b*, Endoh et al. 2014). Ishikawa and Sakai (1981) proposed this concept after reporting the presence of ice formation in bud scales and the simultaneous decrease of floret water content in *Rhododendron* under freezing conditions. Additional studies of an example of freeze-induced dehydration, known as extraorgan freezing, in *Abies firma* (Ide et al. 1998) and *Picea abies* (Kuprian et al. 2017) have reported the progressive freeze dehydration of florets, a lowering of their freezing point, and the subsequent prevention of the formation of lethal intracellular ice. With decreasing temperature, the gradual expression of tissue damage symptoms is, at least in part, related to dehydration (Pearce 2001).

A limited number of studies have evaluated the freezing tolerance status of cranberry terminal buds. Eaton and Mahrt (1977) performed the only reported DTA on cranberry terminal buds with unreliable results due to the extremely fast freezing rates used in their study. Abdallah and Palta (1989) evaluated critical frost killing temperatures of buds by exposing them to a gradient of freezing temperatures during fall and spring and reported a significant gain in freezing tolerance of terminal buds by late October and a loss of hardiness in late April. DeMoranville and Demoranville (1997) and Olszewski et al. (2017) evaluated freezing tolerance of buds during spring by assessing browning in inner bud tissues viewed from a single equatorial cross-section of the buds. Workmaster and Palta (2006) evaluated changes in freezing tolerance during spring by assessing the regrowth capacity of buds subjected to a range of freezing temperatures. The buds of cranberry plants were found to survive temperatures colder than −20 °C following cold acclimation in fall (Workmaster and Palta 2006). Although all these studies have evaluated such shifts in freezing tolerance of cranberry terminal buds, no studies have investigated the freezing stress survival mechanism of cranberry terminal buds.

The objective of this study is to assess the freezing stress survival mechanism of cranberry terminal buds during the dormant period via the study of patterns of freezing stress damage and related processes in specific bud tissues through the use of DTA, controlled freezing tests (CFT), MRI scans, ice nucleation activity (INA) evaluations and histological evaluation of bud structures.

Materials and methods

Site description and plant material

Plant material was collected from three commercial cranberry farms within a 7-km radius in central Wisconsin: Necedah (44°11′14.3″N, 90°04′52.8″W), Cranmoor (44°18′17.2″N, 90°02′22.6″W) and Nekoosa (44°16′46.9″N, 89°55′00.4″W). Upright cuttings of 'HyRed' and 'Stevens,' early and mid-season fruit-ripening cultivars, respectively (Roper and Planer 1993, McCown and Zeldin 2003), were sampled weekly or biweekly from 1 September to 31 December in 2016, 2017 and 2018. 'HyRed' uprights were collected from the Necedah (2016), Cranmoor (2017) and Nekoosa (2018 and 2019) sites, while 'Stevens' samples were collected from the Necedah and Nekoosa sites in 2016 and 2017. On a given sampling date, a total of approximately 400–500 cranberry uprights with dormant terminal buds was collected and transported in sealed plastics bags on ice. Uprights were cut from random locations in each of one-third sections of a bed of dimensions 250 × 50 m as sampling replicates. Samples were processed within 4 h from field collection. Uprights were sorted based on terminal bud size with medium-sized buds (1–2 mm in diameter) selected for DTA and CFT. For a list of collection dates, see Table 1 available as Supplementary Data at *Tree Physiology* Online. In 2015, terminal buds of 'HyRed' were collected from the Necedah site for histological evaluation of bud structures.

Environmental conditions

In 2015, onsite temperature records were not available for the Necedah site. Therefore, daily maximum and minimum temperature records from a Weather Underground network station (ID: KWINECED4, The Weather Company, Brookhaven, GA, USA) (model WS-2090, Ambient Weather, Chandler, AZ, USA) approximately 29 km south of the Necedah site (43°59′34.8″N, 90°00′36.0″W) were used from 1 September to 31 December. For 2017 and 2018, canopy-level air temperatures were monitored at the sites using shielded Hobo pendant data loggers (Onset Computer, Bourne, MA, USA).

Temperatures were recorded at 30-min intervals and later summarized into hourly averages from 1 September to 31 December for each year. The 30-year (1981–2010) average daily minimum temperature for the fall period (1 September to 31 December) and the average first day with temperatures below 0 °C are −1.15 °C and 25 October, respectively, for central Wisconsin (NOAA 2019).

Differential thermal analysis

The DTA was performed weekly in 2016 from 23 September to 12 December ($n = 12$) and biweekly in 2017 from 22 September to 27 November ($n = 5$), using a modified combination of the methodology of Mills et al. (2006) and Einhorn et al. (2011). Thermoelectric modules (TEMs) (model HP-127-1.4-1.5-74 for standard runs and model SP-254-1.0-1.3 for additional testing runs; TE Technology, Traverse City, MI, USA) were used to detect exotherms. The TEMs were placed in individual hinged tin-plated steel containers lined with 5-mm-thick pieces of open-cell foam to reduce air turbulence. Ten TEM units were evenly spaced and attached to each of four 30 × 30 cm perforated aluminum sheet pieces (hereafter called 'trays') and wired to a single 24-pin D-sub connector. A copper–constantan (Type T) thermocouple (22 AWG) was positioned on each of two of the trays to monitor temperature in proximity to the TEM units. Trays were positioned vertically in a Tenney Model T2C programmable freezing chamber (Thermal Product Solutions, New Columbia, PA, USA) and connected to a Keithley 2700-DAQ-40 multimeter data acquisition system (Keithley Instruments, Cleveland, OH, USA). TEM voltage and thermocouple temperature readings were collected at 6-s intervals via a Keithley add-in in Excel (Microsoft Corp., Redmond, WA, USA). The effect of freezing chamber fan turbulence on the TEM units was minimized by covering individual trays with 1.27-cm-thick open-cell foam sheets and by installing a removable piece of perforated corrugated cardboard across the top of the chamber's interior to function as a diffuser.

Terminal buds were excised leaving 5 mm of stem attached with no leaves. Groups of 10 buds lined in rows were wrapped in a small piece of moist paper towel to provide a source of ice nucleation and subsequently wrapped in aluminum foil to form a flat packet. Packets of buds were placed inside the units in direct contact with the TEMs. All freezing runs consisted of a temperature ramp from room temperature to 4 °C, followed by a hold for 0.5 h to ensure equilibration of the system. In 2016, the freezing program continued with a ramp to −30 °C at a rate of 1 °Ch$_{-1}$. In 2017, the freezing program continued with a ramp to −40 °C at a rate of 3 °Ch$_{-1}$.

During the fall of 2017, modifications to the DTA system were made to further test for the detection of exotherms. In a modified DTA methodology based on Wisniewski et al. (1990), two copper–constantan (Type T) microthermocouples (32 AWG) were placed in direct contact with individual cranberry buds to evaluate the relative sensitivity of the TEMs to detect exotherms. The buds with the attached microthermocouples were placed in separate TEM units, as described above. Data collection from the microthermocouples was performed simultaneously with that from the TEMs for 10 buds at each of three freezing chamber runs. Additionally, in the fall of 2017, the alternative model TEM (with the double the number of semiconductor blocks) was used to test for greater sensitivity to a potential exotherm signal.

Controlled freezing tests

The CFT were performed biweekly during the falls of 2017 and 2018 using the methodology of Workmaster and Palta (2006) to induce cold injury in dormant cranberry buds. During the first half of the sampling period (September 22, October 13 and October 27) in 2017, CFT were performed using a Forma Scientific Model 2946 circulating glycol bath (Marietta, OH, USA) under manual temperature control, while for the second half (November 13, November 27 and December 11) of 2017 and all of 2018, CFT were performed in the same programmable freezing chamber used for DTA. Temperatures reached in the glycol bath and freezing chamber were monitored with two copper–constantan (Type T) thermocouples (22 AWG) at different locations within the bath and chamber.

For each CFT, sets of three 10-cm-long cranberry uprights with dormant terminal buds were rinsed with tap water, blotted dry with paper towel and placed in either 70-ml glass tubes with weighted stainless steel caps for the glycol bath or 50-ml plastic centrifuge tubes with plastic caps for the freezing chamber. Five replicate tubes were used at each test temperature, along with a set of five tubes kept on ice as an unfrozen control. The CFT runs in the glycol bath consisted of equilibrating the bath temperature at 1 °C followed by ramping manually at intervals of 1 °Ch$_{-1}$ to −1 °C, at which point a chip of ice was added to each tube and shaken, to promote ice nucleation. Temperature was held at −1 °C for 1 h to allow the system to reach thermal equilibrium. Subsequently temperatures were stepped down from −1 to −6 °C at the 1 °Ch$_{-1}$ interval, followed by a change of cooling interval to 2 °Ch$_{-1}$ until reaching −12 °C, at which point the cooling interval was increased to 4 °Ch$_{-1}$ until reaching the minimum test temperature. In general, the same CFT protocol was followed in the freezing chamber, with the exception of the use of auto-running freezing programs with ramped temperature decreases of 1, 2 and 4 °Ch$_{-1}$ and the inducement of ice nucleation by firmly shaking the racks of screw-cap tubes during temperature equilibration at −1 °C.

Tubes were removed from the glycol bath or freezing chamber at eight test temperatures in 2017 ranging from 0 to −20 °C for the first three sampling dates, 0 to −30 °C for the fourth sampling date and 0 to −40 °C for the last two dates. In 2018, the minimum temperature ranged from −24 to −40 °C in September and October and to −50 °C in November and December. Once removed from the freezing environment, tubes

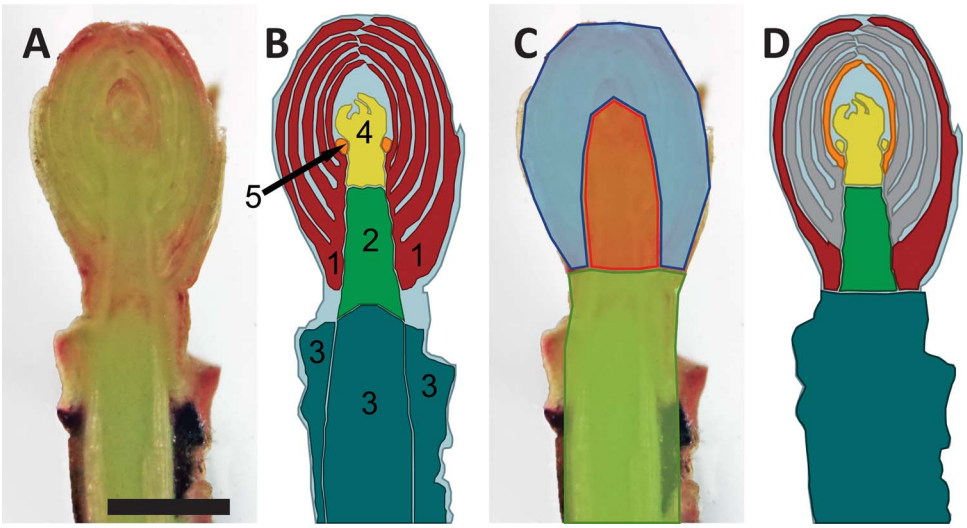

Figure 1. Longitudinal section of the cranberry reproductive terminal bud and diagrams of bud structures and ROI defined for the studies presented. (A) Fresh longitudinal section. (B) Anatomical structures evaluated for freezing stress damage: red = bud scales; green = bud axis; dark cyan = stem section; yellow = SAM; and orange = flower primordia. (C) Defined ROI for MRI analysis: orange = inner bud; blue = outer bud; green = stem. (D) Bud tissues excised for INA assay: red = outer bud scales; orange = most inner bud scales; gray = unused bud scales; yellow = flower primordia/SAM; green = bud axis; dark cyan = stem. Scale equals 1 mm.

were kept on ice in the dark for 12 h, after which samples were kept for 3 days at 4 °C in the dark to allow for recovery of injured tissues. Before bud damage evaluation, samples were held for 24 h at room temperature in low light conditions to ensure maximal symptom expression in bud structures.

Bud damage evaluation

Buds from the CFT were dissected for freezing damage assessment and documented using an Olympus SZX12 dissection microscope with a 1x objective (Olympus Optical Company, Tokyo, Japan) connected to a Canon EOS Rebel T6i digital camera (Canon U.S.A., Inc., Melville, NY, USA). Buds were cut longitudinally with a double-edged razor blade and immediately observed for browning distribution and severity. Freezing damage was assessed by the evaluation of multiple bud or related structures: bud scales, shoot apical meristem (SAM), flower primordia, bud axis and the attached stem section (Figure 1A and B). Each structure was evaluated independently for the severity of oxidative browning (Larsen 2009) and water-soaked appearance and rated by a discrete scale with four levels of damage from 0 to 3, with 0 being no damage and 3 complete damage (Figure 2).

Histological observation of bud structures

In the fall of 2015, and in conjunction with a bud flower primordia study (Bolivar-Medina et al. 2018), sets of five uprights were sampled on three different dates: 11 September when fruit were mature; November 9, post-harvest and early dormancy; and 29 December when buds were maximally dormant (immediately prior to the conventional grower practice of strategically timed flooding of production beds for the formation of protective layers of ice ('winter flood')), to evaluate changes in bud development. Sample preparation was performed as described by Bolivar-Medina et al. (2018). Briefly, for every sampling date, terminal buds were excised with a 5-mm stem portion attached and leaves removed and then fixed in a solution of glutaraldehyde (Sigma-Aldrich, St Louis, MO, USA) overnight at 4 °C and then rinsed in a 0.05 M potassium phosphate buffer and dehydrated in a graded ethanol series. Subsequently, samples were slowly embedded by gradual replacement into medium-grade LR white resin (Ted Pella, Inc., Redding, CA, USA). Once samples in resin were polymerized at 60 °C for 28 h, they were mounted on stubs and sectioned longitudinally (2 µm thickness) on a Sorvall MT-2 ultramicrotome (Ivan Sorvall, Norwalk, CT, USA). Thin sections were collected and mounted on Fisher Probe-On-Plus slides (Thermo Fisher Scientific, Waltham, MA, USA), stained with 0.05% (w/v) Toluidine Blue O (Sigma-Aldrich) and coverslips annealed with Cytoseal 60 (Thomas Scientific, Riverdale, NJ, USA). All observations were done on a bright field Olympus BX50 microscope (Olympus Optical Company). The objectives used included Plan Apo 10x and 40x. Images were captured with the digital camera system described above.

Magnetic resonance imaging

Magnetic resonance imaging of cranberry buds collected from 7 November 2018 (Nekoosa site) was performed using the methodology described by Villouta, C., Cox, B., Rauch, B., Workmaster, B.A., Eliceiri, K. and Atucha, A. (in preparation) within 24 h of field collection. Buds of diameter 1–2 mm were selected for imaging. A single set of 28 buds were placed in

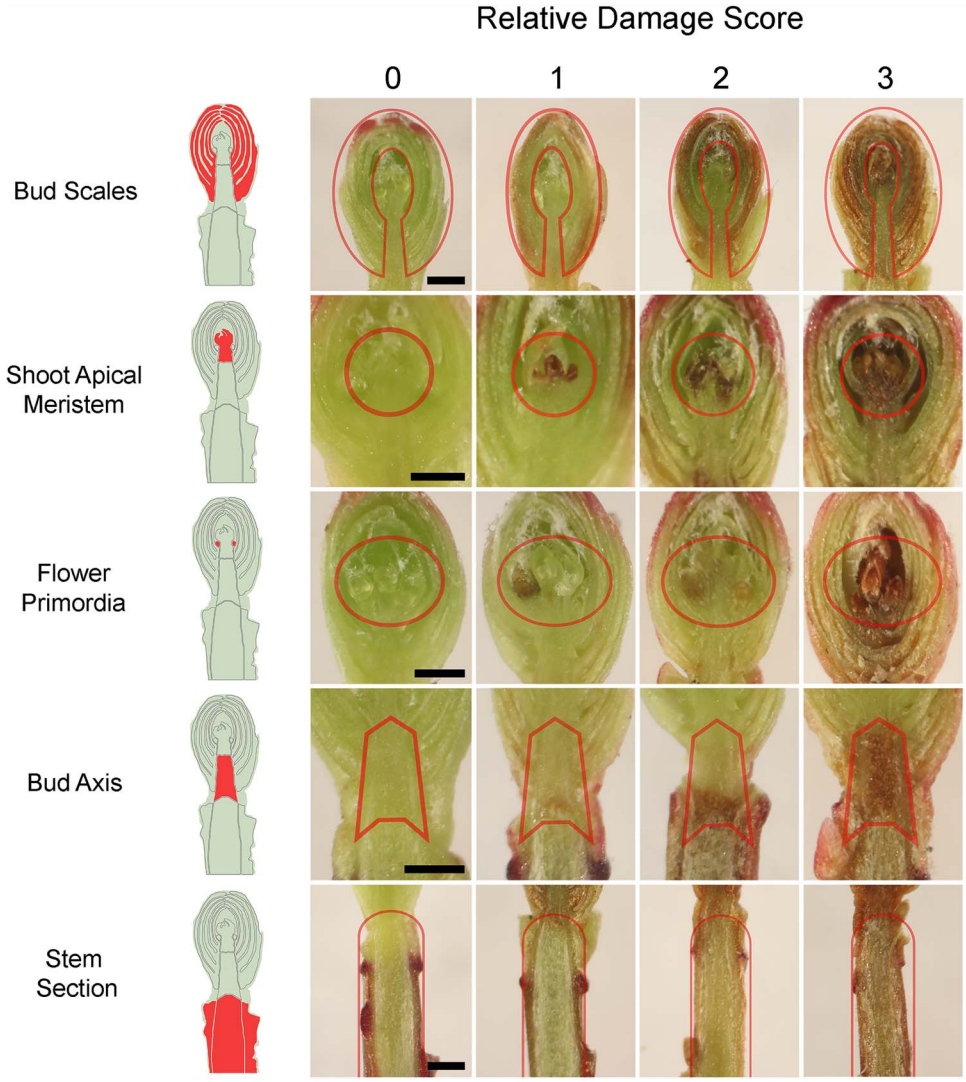

Figure 2. Representative images of CFT-induced freezing stress damage in cranberry reproductive terminal buds sampled in the fall of 2018 from a commercial farm near Nekoosa, WI. Damage in different bud structures was scored on a relative scale of four discreet levels from 0 to 3, with 0 being no damage to 3 being total damage. The CFT freezing rate was 4 °Ch_{-1}. Red lines delimit the evaluated area for each structure. Scale bar 0.5 mm.

a custom-made MRI-compatible freezing chamber connected to a circulating ethylene glycol cooling system (Villouta et al. in preparation).

Magnetic resonance imaging was performed in a Varian 4.7-T small animal imaging system (Agilent Technologies, Palo Alto, CA, USA). Image acquisition was performed with a spin echo multi-slice pulse sequence. Ten 1-mm-thick slices were acquired with a field of view of 30 × 30 mm. Each slice was scanned 23 times with the following capture parameters, 512 × 512 pixels matrix, TE 21.5 ms, TR 306.4 ms for a total acquisition time of 52 min per temperature treatment (20, −7, −14 and −21 °C).

The MRI run consisted of equilibration of the sample chamber for 20 min at each treatment temperature and holding for the duration of the image acquisition. After the 20 °C image acquisition, the chamber temperature was ramped to −1 °C at a rate of 10 °Ch_{-1} and held for 1 h. Subsequently the rate of cooling between each treatment temperatures was 3 °Ch_{-1}.

Images were visualized with Multi FDF Opener package for ImageJ (Schneider et al. 2012). Window and level settings were normalized for each image. The mean gray values (MGV) of individual buds were evaluated for comparing the different proton signal saturation for individual buds at each temperature. Areas of higher MGV (brighter) are associated with higher densities of mobile protons, primarily from liquid water, while areas of lower MGV (darker) are associated with sources of lower densities of mobile protons, including frozen water. Three regions of interest (ROI) in the buds were defined for comparison across temperature treatments: outer bud, inner bud and stem, which generally correspond to the structures defined for CFT damage evaluation (Figure 1C). The MGV for the background was calculated at each temperature and

subtracted from the intensity (MGV) values of the three ROI at the respective temperatures.

Evaluation of INA

Ice nucleation activity in cranberry terminal buds was performed within 24 h of sample collection from the field on October 15, 2019
(Nekoosa site), using a test tube assay methodology (Ishikawa et al. 2015). Forty buds of diameter 1–2 mm were selected. To eliminate contaminating nucleators, all instruments and materials were autoclaved at 121 °C for 21 min, and dissections and sample preparation took place in a laminar flow chamber. Buds were dissected and separated into five tissue types: outer bud scales, the most inner bud scales, embryonic shoot (including flower primordia and shoot apical meristem), bud axis and stem (Figure 1D). Each tissue type excised from each bud was placed in a new 6-ml borosilicate glass tube (Fisher Brand, Houston, TX, USA) containing 300 µl of 0.1-µm-filtered molecular biology grade water (BP2819-4, Thermo Fisher Scientific). Forty replicates of each evaluated tissue type were used. A single rack holding all the tubes was covered with a rectangular piece (25 × 12 cm) of 5-mm-thick clear acrylic (Acrylite FF, Cyro, NJ, USA) that was attached to the rack by rubber bands. The prepared rack of tubes was weighted with stainless steel discs and placed in the same circulating glycol bath used for CFT and submerged to 3 cm of the tubes' height. The temperature of the glycol bath was monitored by two copper–constantan (Type T) thermocouples (22 AWG). The INA runs consisted of equilibrating the bath temperature at 4 °C followed by setting the bath temperature to reach 0 °C in 25 min. The evaluated temperatures were 1 °C intervals from 0to −20 °C. After each 1 °C decrement, equilibration was reached in 5 min and then followed by a hold of 20 min. At the end of each 20-min hold, the phase state of the water in each tube was evaluated by observation through the acrylic cover. To facilitate this, tubes were illuminated from above with a flashlight. The INA was reported at each temperature as the cumulative number of frozen tubes. To compare relative differences of INA across the tissue types, the median ice nucleation temperature (INT) was expressed as the temperature at which 50% of samples froze, as determined by Ishikawa et al. (2015). The variance of the median INT was expressed as ±SD, tabulated as the range when two-thirds of the INT values are within 1 SD (Ishikawa et al. 2015).

Results

Environmental conditions

In 2015, daily minimum and maximum temperatures (as recorded at the nearby Weather Underground station) trended regularly downward over the fall to early winter (Figure 3A). Daily minimum temperatures did not fall below 0 °C until 14 October, and from that point until late November, daily minimum temperatures were greater than −5 °C. From late November until the end of 2015, there were three instances where the daily minimum temperature dropped below −10 °C for multiple days.

In 2017 and 2018, cranberry canopy-level air temperatures were similar from September to December 7 (Figure 3B and C). However, in the latter half of December 2018, minimum temperatures were warmer than those experienced in 2017, delaying the timing of the grower's 'winter flood' practice for extreme temperature protection, thereby extending our access to plant material through the end of the year. Winter flooding for ice formation was performed on 9 December and 8 January in 2017 and 2019, respectively. The first subzero daily minimum temperatures in 2017 and 2018 were recorded on 16 October and 29 September, respectively, 9 and 26 days earlier than the 30-year average daily minimum temperature in this region (NOAA 2019).

Differential thermal analysis

During 2016, a total of 12 DTAs were performed with dormant buds of 'HyRed' and 'Stevens'. For each DTA, high-temperature exotherms (HTEs) were recorded (Figure 4), indicating the freezing of the included moist towel piece, as well as any free water in the samples, presumably including the formation of extracellular ice in the plant tissues. However, no low-temperature exotherms (LTEs) were detected in any DTA run to indicate the nucleation of intracellular ice in supercooled tissues. During the fall of 2017, five DTAs were performed, but similar to 2016, no LTEs were detected, even with the use of the alternative model TEMs or microthermocouples attached to individual buds.

Controlled freezing tests

From the CFT curves, it was possible to identify the coldest temperature at which damage symptoms were comparable to the control. This temperature shifted across the season each year (Figure 5). For several of the later sampling dates in 2017, this temperature value could not be defined because the lowest test temperature did not result in damage greater than the control. Despite this, comparisons of susceptibility to damage were done between years, when possible. As a general trend, 2017 CFT showed damage expression at lower temperatures than a similar date in 2018, until mid-October when the trend was inverted. Comparison of bud structure damage between years was not possible after mid-November due to the lack of damage observed in CFT during 2017.

In detail in 2018, the temperature at which damage severity started to increase was −10 °C on September 20, which then decreased to −24 °C by 1 November, and subsequently stayed constant until the last sampling date, December 27. Considering all of the bud structures, maximum damage was

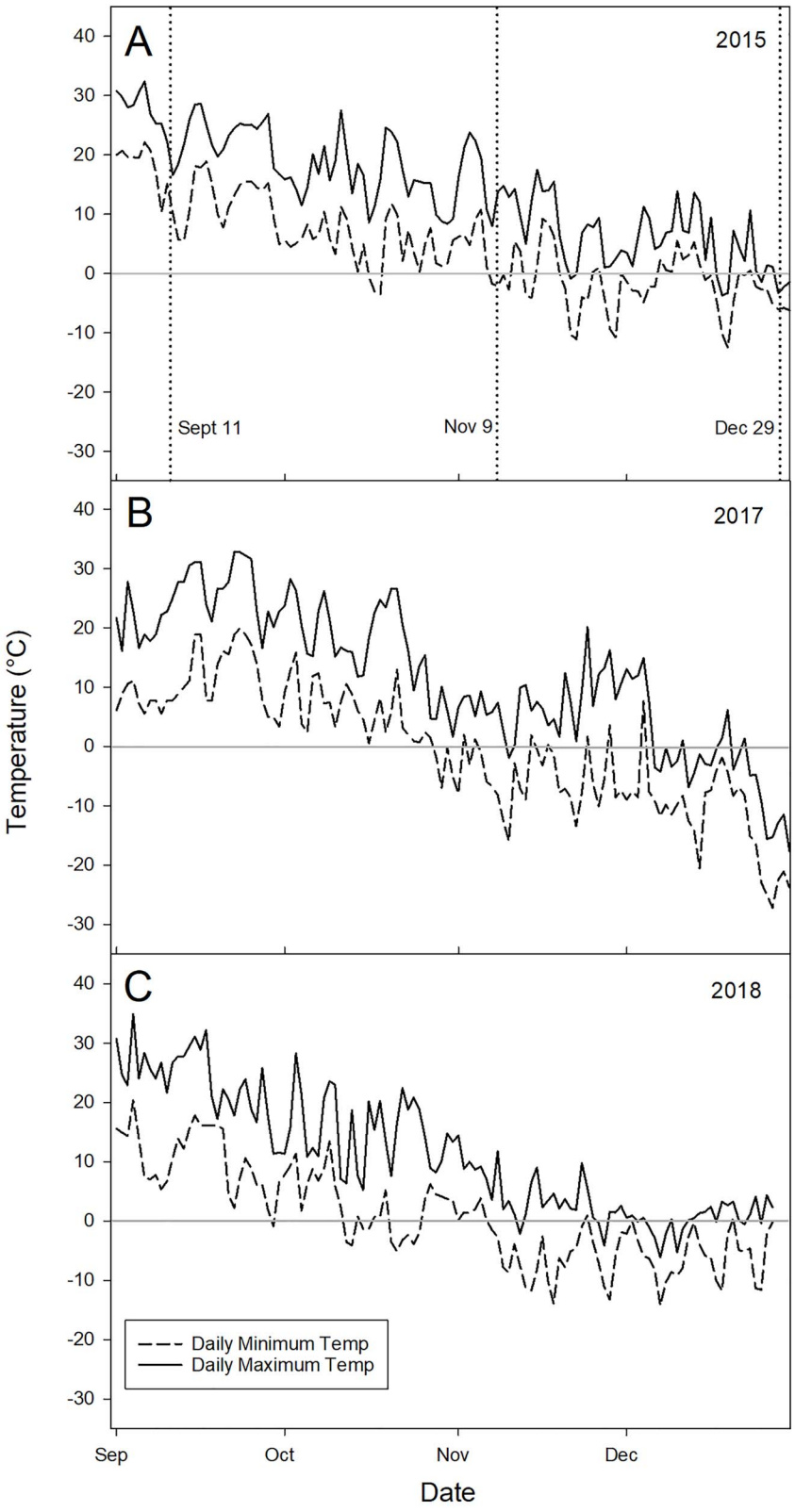

Figure 3. Daily minimum and maximum air temperatures from 1 September to 31 December in 2015, 2017 and 2018 (A–C, respectively). In 2015 (A), ambient air temperature data was collected from a weather underground network station (ID: KWINECED4) approximately 29 km south of the Necedah site (43°59′34.8″N, 90°00′36.0″W). Vertical dotted lines denote each sampling date for bud histology. In 2017 (B) and 2018 (C), air temperature data was recorded by the researchers at a commercial cranberry farm near Nekoosa, WI (44°16′46.9″N, 89°55′00.4″W), 1 m above the canopy on the side of the surrounding dike on the long side of the bed. The central horizontal line in each plot denotes 0 °C.

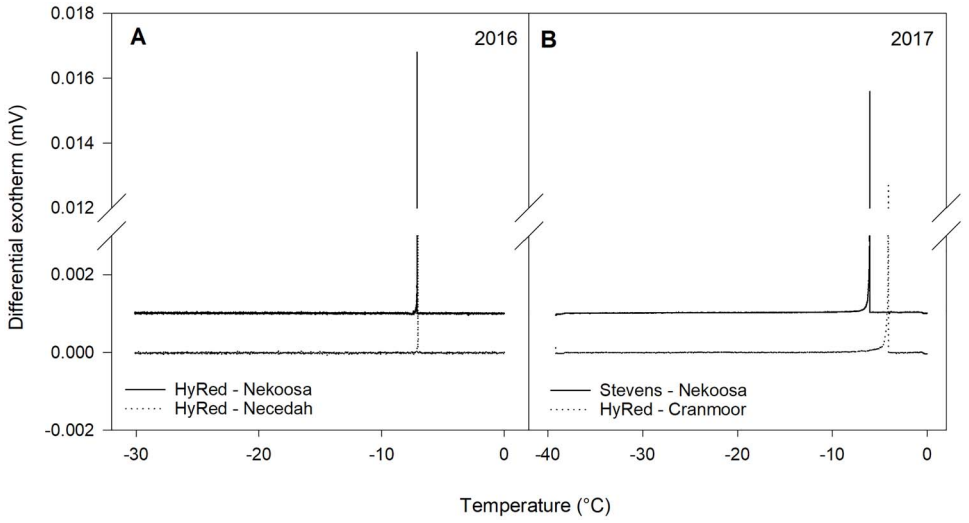

Figure 4. Examples of DTA output plots from the testing of reproductive cranberry terminal buds in November 2016 and 2017. The peaks depicted in each plot are the HTEs. No LTEs were observed. Samples collected from different commercial cranberry farms were evaluated: (A) November 2016, 'HyRed' buds from Nekoosa and Necedah, WI, and (B) November 2017, 'Stevens' buds from Nekoosa and 'HyRed' buds from the Cranmoor area, WI.

observed in the first sampling dates within a shorter span of temperatures, compared with later sampling dates. For example, on 20 September damage was initially noticeable at −10 °C, and the highest severity was reached at −24 °C, while on 27 December, damage was initially seen at −24 °C, with the highest damage reached at −50 °C.

A range of damage severity was observed in different bud structures over the sampling period (Figure 6). In September, bud scales and bud axis structures incurred higher levels of damage compared with flower primordia, SAM and stem sections, while in the immediately following sampling dates, the stem section and bud axis structures had the highest degrees of damage. In contrast, bud scales and SAM became the structures incurring some of the lowest levels of damage from mid-October to the end of the sampling period. Overall, the spread of damage severity among the bud structures was wider in the latter part of the season. Differences in damage severity between 'Stevens' and 'HyRed' were only observed in the 27 November 2017 sampling date, when 'Stevens' incurred greater damage at the lowest tested temperatures.

Histological evaluation of bud structures

Flower primordia were present by the first bud collection date for histological preparation (11 September 2015) (Figure 7A). Changes in the integrity of bud scale tissue were observed between the second and last collection dates (9 November and 29 December 2015). Separations between the first and second layers of mesophyll cells of both the adaxial and abaxial sides of each bud scale were observed in samples from the 29 December collection. However, no disruptions in the vascular connections between the base of bud scales and the bud axis were observed.

Magnetic resonance imaging

The slices obtained from the MRI did not yield uniform central longitudinal sections for all 28 buds, due to differences in positioning of the buds in the sample holder tubes. Instead, the best defined central sections of 14 buds were imaged and used for evaluation. The resolution of images obtained from MRI scans did not allow for the identification of specific tissues (Figure 8A–E); however, there was sufficient resolution for the identification of macro ROIs for comparison of relative MGVs. Buds scanned at 20 °C had a lower relative amount of water in the outer bud region (represented by a lower MGV) as compared with the inner bud region, which had the highest relative amount of water of the three ROIs (Figure 8G). When temperature decreased to −14 °C, the outer bud MGVs reduced to zero. A significant reduction in MGV was observed in the inner bud region, with smaller relative changes in the stem and outer bud regions. At −21 °C the inner bud MGV was lower than at −14 °C, only slightly greater than that of the outer bud region. In contrast, the stem region MGV remained more consistent over the course of the experiment.

Signal intensity (shown as MGV) increased somewhat at −7 °C. The sensitivity of detection in MRI increases with temperature decrease as an effect of differences between nuclear energy levels (Price et al. 1997*a*), as described by the Boltzmann distribution (Goldman 1988). This variation in intensity is negligible in comparison with the changes detected once water freezes, a phenomenon that has been observed in previous studies of plant material (Price et al. 1997*a*, Ide et al. 1998).

Ice nucleation activity

The evaluated tissue types had similar patterns of INA; however, they were notably different from each other (Figure 9). The

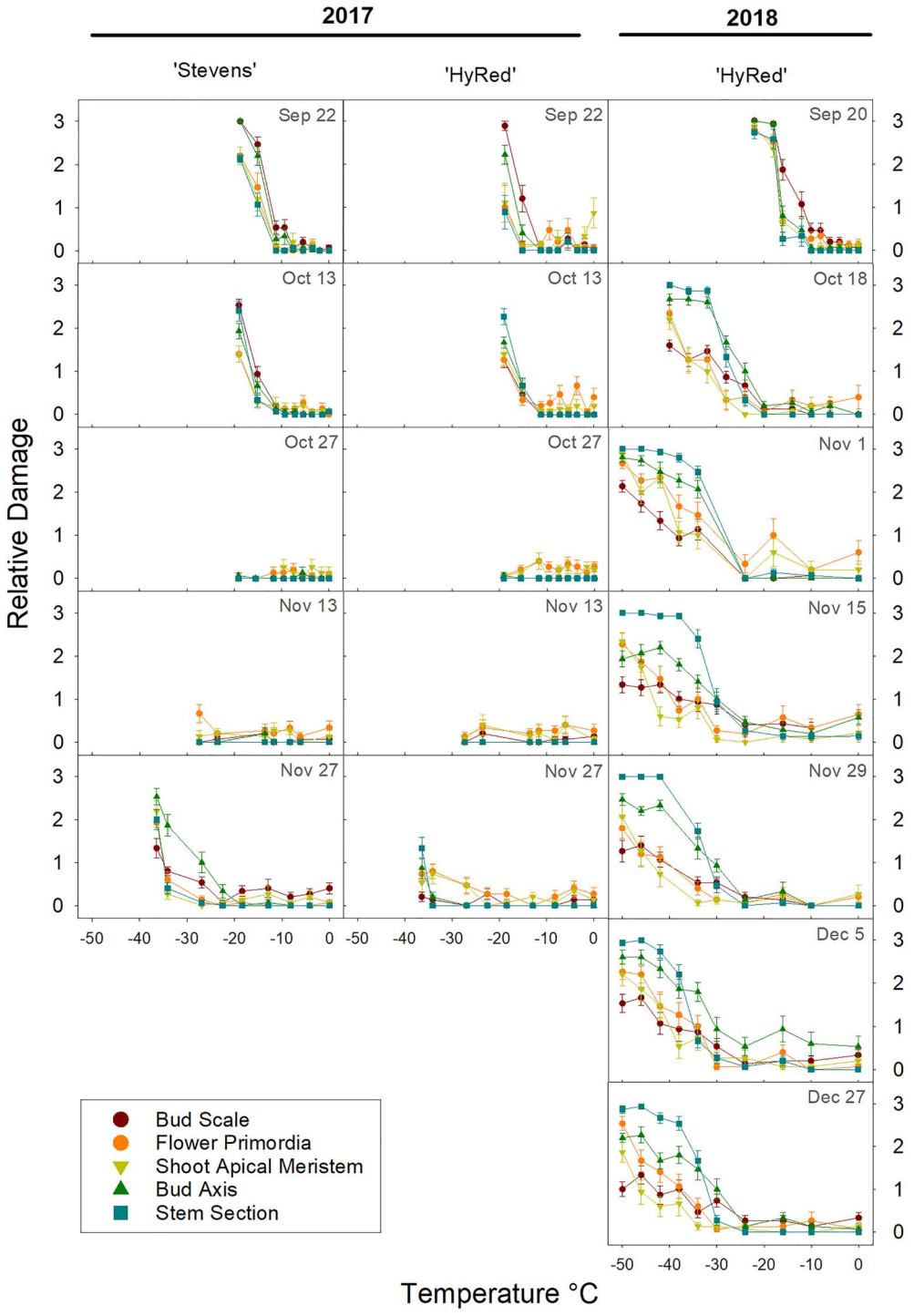

Figure 5. Seasonal changes in CFT-incurred damage by bud structure in 'Stevens' and 'HyRed' reproductive cranberry terminal buds sampled from a commercial farm near Nekoosa, WI, in the fall of 2017 and 2018. Plot columns for 2017 depict results for the two cultivars. In 2018, only 'HyRed' was sampled. Rows depict sampling dates within one calendar week. Relative damage is a discrete scale with four levels of damage from 0 to 3, with 0 being no damage and 3 complete damage. Each point represents the average damage score for a given structure ($n = 15$). Vertical bars represent the standard error of the mean.

temperature of initiation of nucleation activity across the tissue types ranged between −4 and −7 °C and did not occur until −8 °C for distilled water. The cumulative curves for all tissues were sigmoidal (Figure 9A). Stem and bud axis tissues had higher median INT values of −6.3 and −7.1 °C, respectively (Figure 9B), reflecting their higher INA. In contrast, the combined tissues of flower primordia/SAM had the lowest median INT value (−10.9 °C) of all the tissue types. The most inner

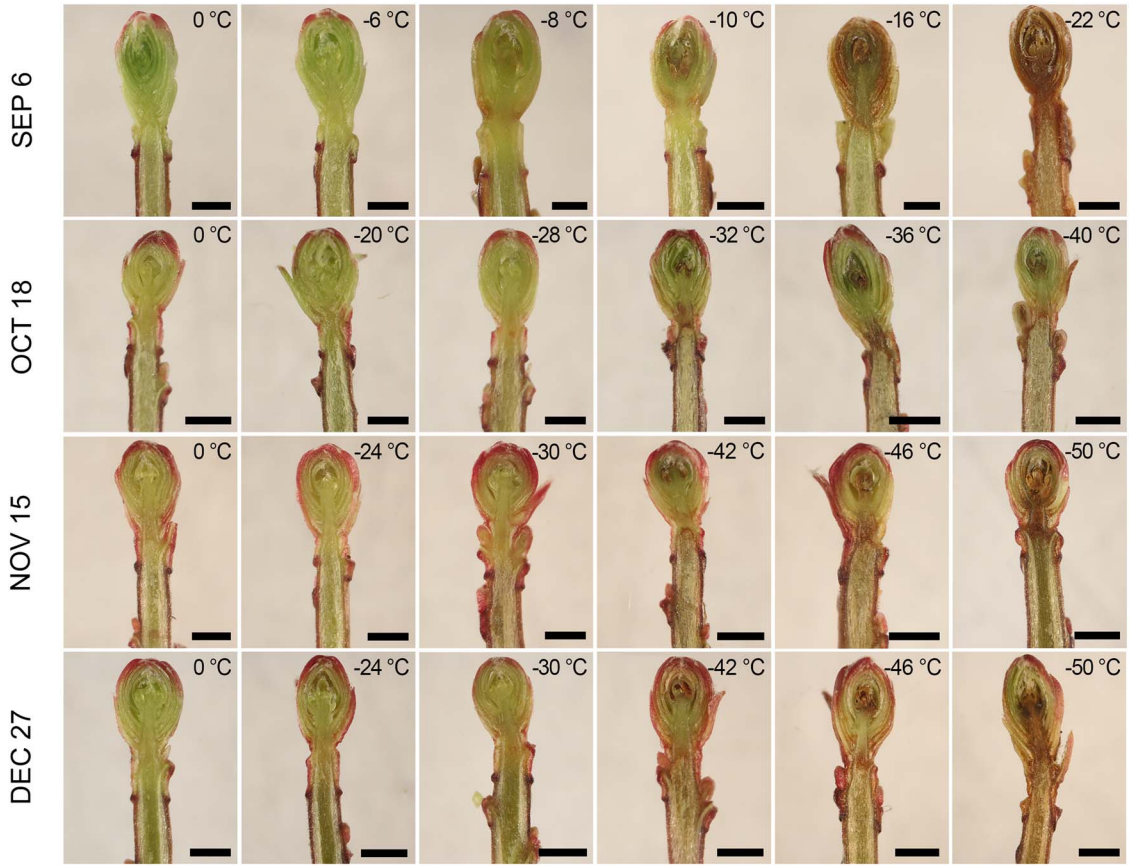

Figure 6. Distribution and range of damage severity in longitudinal dissections of 'HyRed' reproductive cranberry terminal buds subjected to CFT across four sampling dates in the fall of 2018. Buds were sampled from a commercial cranberry farm near Nekoosa, WI. Each row represents a single CFT performed on that date. Each picture includes the minimum temperature to which that bud was exposed at a freezing rate of 4 °Ch$_{-1}$. Scale bars 1 mm.

bud scales had a similar level of INA as flower primordia/SAM, with a median INT of −10.2 °C. The cumulative curve for the outer bud scales was intermediate to those of the other tissue types, with an INT value of −8.3 °C. The control tubes with only filtered molecular biology grade water had the lowest median INT of −18.5 °C. Although the INA of the flower primordia and the SAM may differ, the extremely small size of these tissues made dissection challenging, and it was concluded that these structures should be considered together.

Discussion

The main objective of this study was to determine the freezing stress survival mechanism of cranberry terminal buds. Evidence gathered in this study supports the interpretation that cranberry terminal buds survive extended periods of freezing stress by a strategy involving freeze-induced dehydration.

Inner tissues of cranberry terminal buds do not supercool

For multiple seasons, LTEs were not detected in DTA or microthermocouple testing (Figure 4). A previous attempt to evaluate the freezing tolerance of cranberry terminal buds in spring using DTA (Eaton and Mahrt 1977) reported a correlation between visual bud tissue damage and the average temperature of the exotherms recorded. However, their results were problematic due to their use of an unrealistic freezing rate of 20 °C min$_{-1}$. Rates this extreme are known to artificially shift exotherms to lower temperatures (Quamme 1995) and are not rates observed in nature (Steffen et al. 1989) and thus are not recommended for use in freezing stress resistance studies. In addition, their reported exotherms were not identified as HTEs or LTEs, and it is plausible they could have been solely from the freezing of extracellular water typically associated with HTEs.

The detection and verification of LTEs in deep supercooling buds require the utilization of appropriately sensitive measurement equipment, as well as realistic experimental parameters. Given the relatively small size (1–2 mm diameter) of cranberry terminal buds, we took significant measures to address technical aspects potentially impeding the detection of LTEs. Alternative TEMs with double the number of semiconductor blocks were evaluated duplicating the probability of detecting heat release but did not increase voltage signals related to freezing events relative to background noise. In addition, background noise in the data output was minimized by controlling freezer fan

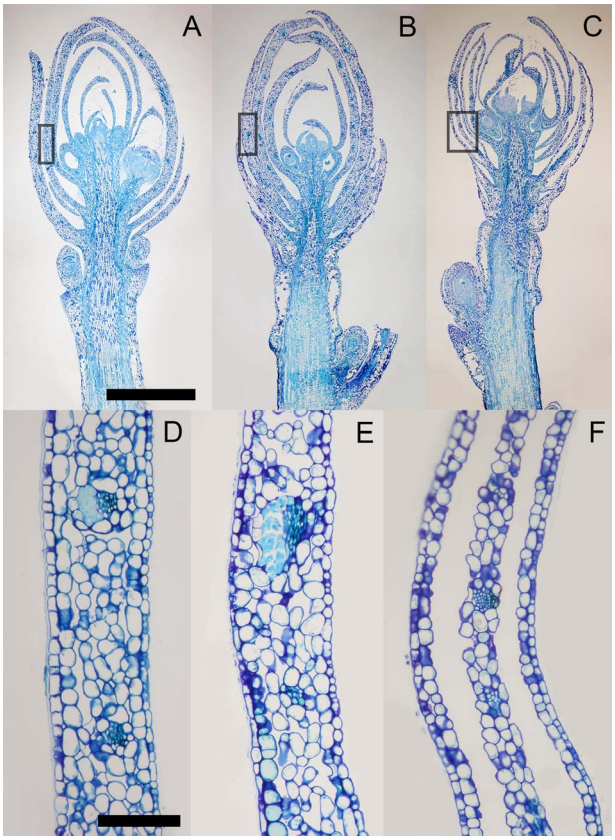

Figure 7. Morphology of cranberry reproductive terminal buds depicted in longitudinal sections. (A–C) Buds were sampled on September 11, November 9 and December 29, 2015, respectively, from a commercial cranberry farm near Necedah, WI. (D–F) Close-ups of the outermost full bud scale, outlined in the black rectangle areas in A–C, respectively. Buds were sampled at three different physiological states of the plants: (A) fruit maturity, (B) initiation of endodormancy and (C) endodormancy. Scale bars A–C, 1 mm; D–F, 100 µm.

turbulence through the installation of a diffuser and by covering the DTA trays with 1.27-cm open-cell foam. Additional testing by adhering microthermocouples directly to bud scales and stems (Wisniewski et al. 1990) also did not yield any LTEs.

Our findings from the DTA are consistent with the MRI scan results showing the lack of supercooled structures in the inner bud area as temperature decreased. In previous similar MRI studies, the inner structures of buds of woody plant species undergoing deep supercooling remain distinctively unfrozen in comparison with the rest of the bud (Ishikawa et al. 1997). In contrast, in our study the partial reduction in MGV observed for the inner bud area at −14 °C was followed by an essentially complete reduction of signal at −21 °C and occurred over the temperature range when no damage was detected in the CFT. This observation is consistent with a gradual reduction in the content of liquid water. In addition, in the INA study, the cumulative pattern of ice nucleation for the combined flower primordia and SAM tissues was sigmoidal, similar to the other structures. Considering the improvements to the DTA setup, the lack of detection of LTEs, coupled with the MRI and INA results, it is reasonable to conclude that cranberry terminal buds do not utilize deep supercooling of sequestered amounts of water as a freezing stress survival mechanism.

Support for interpretation of the process of freeze dehydration

The process of freeze-induced dehydration in woody plant buds involves the gradual dehydration of the inner bud tissues, driven by the establishment of a vapor pressure deficit gradient created by the presence of extracellular ice in bud scales (Sakai 1979, Ishikawa and Sakai 1981). In this process, inner bud tissues such as flower primordia and the SAM can withstand a substantial loss of water to the bud scales, thus avoiding the formation of lethal intracellular ice. Previous studies (Ishikawa 1982, Price et al. 1997*b*, Ide et al. 1998) state that the role of bud scales is characterized by their capability of freezing at relatively warmer temperatures in comparison with the other bud structures. In our study evidence for the establishment of the freeze dehydration process from the INA study and MRI scans occurred between 0 and −21 °C, a temperature range over which no damage was detected in CFT evaluations for any structures of fully cold hardy buds.

Ice nucleation activity assays of excised bud tissues test the relative probability of nucleation for different bud structures. In our study, outer bud scales had a cumulative pattern of nucleation occurring at warmer temperatures than the most inner bud scales and flower primordia/SAM (Figure 9A). This INA behavior has been reported for other ericaceous species, such as *Rhododendron japonicum* (A. Gray) Suringer, where bud scales had a warmer median INT compared with flower primordia/SAM (Ishikawa et al. 2015). In the MRI scans, bud scales had a drastic reduction in their relative amount of liquid water, suggesting their complete freezing by −14 °C, a state reached before other structures.

The formation of icicles in bud scales has been reported in buds that successfully undergo both deep supercooling (Quamme 1978) and extraorgan freezing (Ishikawa and Sakai 1981, Pearce 2001, Wisniewski et al. 2014) without compromising bud survival (Ashworth 1990, Flinn and Ashworth 1994*b*). In longitudinal sections of buds sampled in early winter (29 December 2015), we observed voids between the first two mesophyll cell layers of bud scales (Figure 7) in all of the buds sampled at a date by which there had already been three instances of the daily minimum temperature dropping below −10 °C for multiple days (Figure 3A). None of the buds sampled prior to this (November 11) had these distinct voids present in their bud scales. These plants had experienced temperatures below freezing, but the daily minimums were above −5 °C. Although we did not directly observe ice crystal formation in bud scales, we posit that these voids are most likely

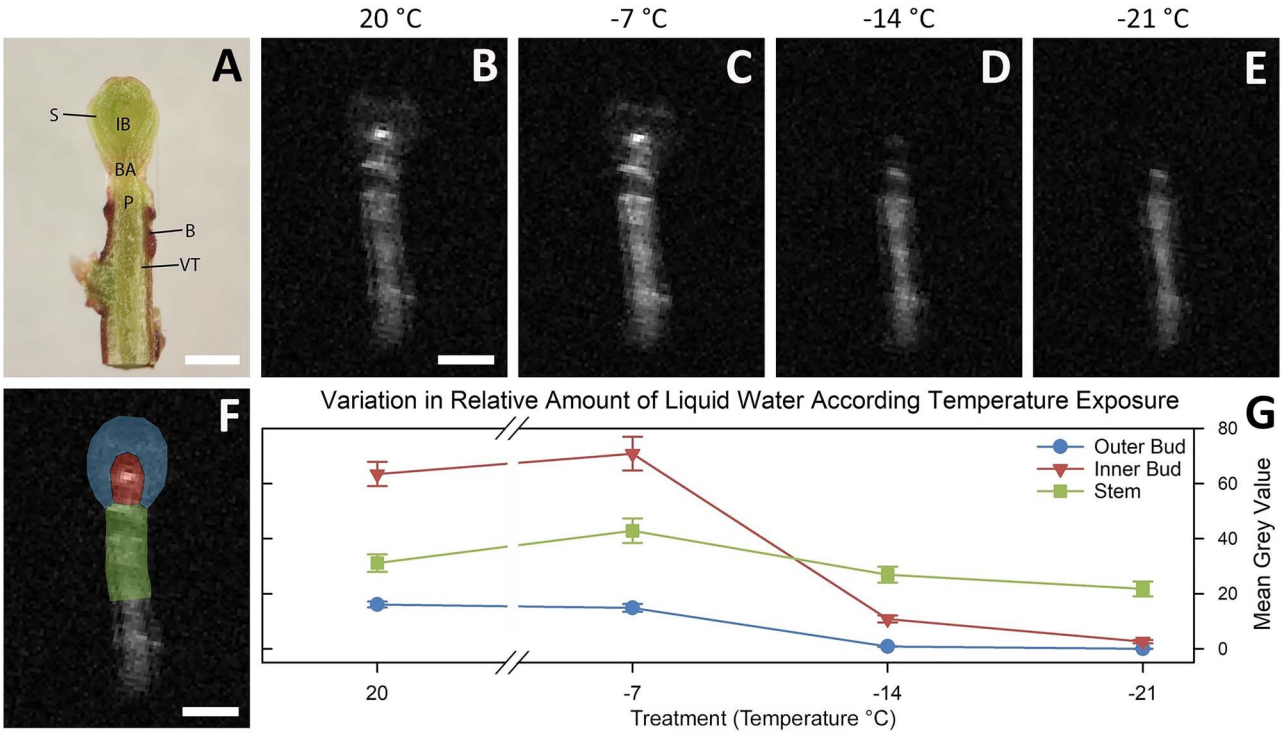

Figure 8. Results of MRI of cranberry terminal buds at a range of freezing temperatures with the use of a custom-made MRI-compatible freezing chamber connected to a circulating ethylene glycol cooling system. (A) Fresh longitudinal section of cranberry terminal buds collected in November, 2019, observed by dissection microscope with main anatomical features noted: B = bark; BA = bud axis; IB = inner bud (shoot apical meristem and flower primordia); S = scale; VT = vascular tissue; P = pith. (B–E) Magnetic resonance imaging longitudinal slices of excised buds at evaluated freezing temperatures, 20, −17, −14 and −21 °C, respectively. Images are enlarged from a MRI acquisition of 20 averages with a field of view of 30 × 30 mm with 532 × 532 pixels. Light portion of images indicates the presence of water in liquid state. (F) Magnetic resonance imaging longitudinal slice of excised bud with ROI for mean gray value calculations highlighted: blue = outer bud; red = inner bud; green = stem. (G) Plot of changes in mean MGV by ROI and evaluated temperatures. Error bars denote standard error (n = 14). Scale bars equal 1 mm.

the vestiges of repeated and extended periods of extracellular ice formation.

The SAM and flower primordia had the coldest median INT, reflecting a relatively low INA. Water translocation from flower primordia to bud scales may occur through vascular traces or via the intercellular spaces between neighboring parenchyma cells (Ishikawa and Sakai 1985). In examples of species that survive by extraorgan freezing, a type of freeze dehydration, such as *Rhododendron* spp. (Ishikawa and Sakai 1981), the level of freezing tolerance in buds has been related to the rate and degree of desiccation of flower primordia. In the MRI study, the MGV of the inner bud structures had two levels of signal reduction: a partial decrease from −7 to −14 °C, followed by a near total reduction at −21 °C. These observations are indicative of a progressive reduction in the relative amount of liquid water in the inner bud structures. This phenomenon has been observed also in *Abies firma* Sieb. et Zucc. (Ide et al. 1998) and described as a potential process of freeze dehydration.

The role of the bud axis in freeze dehydration has been described as being part of the water mobilization path through intercellular spaces and vascular tissue traces. Studies in blueberry (Flinn and Ashworth 1994*a*), *Cornus officinalis* (Ishikawa and Sakai 1985) and larch (Endoh et al. 2014) found that the subtending bud tissue contributed to the avoidance of intracellular ice formation in the bud primordia by functioning as an avenue for water migration to the bud scales. In the INA study, the bud axis had one of the highest median INT values, surpassed only by that of the stem. By experiencing ice nucleation earlier than other bud structures, the bud axis may likely play a coordinating role with the bud scales in the establishment of the vapor pressure deficit gradient. The presence of a physical barrier in the bud axis may play an additional role in the freezing stress resistance mechanism of the bud by limiting the ice propagation from the stem, although this aspect has not yet been explored in cranberry.

Freezing and dehydrative damage at extremely low temperatures (<−20 °C)

Once the tolerance threshold of a freezing temperature survival strategy of a plant tissue or organ is overcome by low temperatures, damage symptoms arise. In the present study, after buds attained maximal freezing tolerance in November, tissue browning at levels above the control were observed at −20 °C and

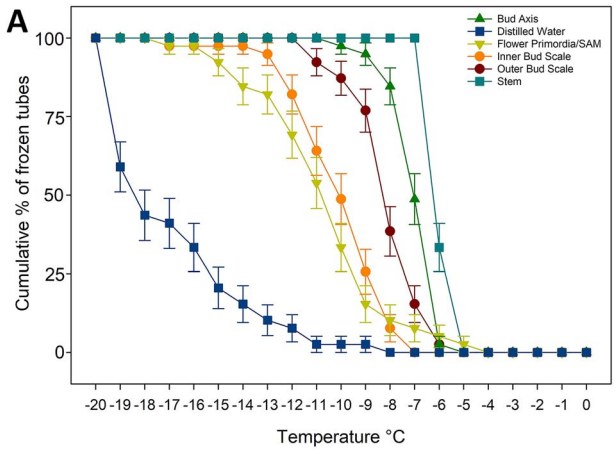

B

Evaluated Structure	BA	DW	FP/S	IBS	OBS	ST
Median INT (°C) ± SD	-7.1 ± 0.8	-18.5 ± 2.6	-10.9 ± 2.5	-10.2 ± 1.9	-8.3 ± 1.3	-6.3 ± 0.6

Figure 9. Ice nucleation activity of excised cranberry terminal bud structures. Assay was performed in a circulating glycol bath. One specimen of each structure was placed in a glass tube with 0.3 ml of 0.1 µm autoclaved filtered molecular biology grade. (A) Cumulative plots by bud structure of percentage of frozen tubes (n = 40 per bud structure) with temperature decrease from 0 to −20 °C. Error bars represent the standard error of the mean. (B) Median INT values for all the evaluated structures and the control: BA = bud axis; DW = distilled water (control); FP/S = flower primordia/SAM; IBS = inner bud scales; OBS = outer bud scales; ST = stem. The SD of the median represents when two-thirds of the INT values are within 1 SD range.

increased gradually as test temperatures decreased (Figure 6). However, for the SAM and flower primordia, maximum levels of tissue browning were rarely observed. In contrast, when buds undergo deep supercooling, and the temperature threshold of freezing resistance is surpassed, a fast and lethal intracellular ice nucleation occurs, and ice is quickly propagated throughout the internal bud tissues (Quamme 1974, George et al. 1974*b*, Quamme et al. 1995), including flower primordia, SAM and inner bud scales.

While all bud structures had a marked shift in hardiness by early November, the levels of tissue browning resulting from the imposed freezing stress of the CFT varied across structure type and were observed over both years and across all sampling dates. In September, bud scales incurred the highest degrees of tissue browning at relatively warmer freezing temperatures (Figure 5). This is likely the result of the lack of acclimation of bud scale cells in early fall to tolerate the biophysical stresses of extra cellular ice, whereas by mid-October through December, bud scales have acclimated and are able to withstand these stresses. These acclimation changes might involve an increase in concentration of amino acids, certain sugars and dehydrins that allow the cells to cope with the dehydrative stress from extracellular ice formations (Koster and Lynch 1992, Welin et al. 1994, Danyluk et al. 1998, Wanner and Junttila 1999, Pearce 2001).

The stem section had one the highest incidences of tissue browning in response to the imposed freezing stress once buds became hardy (Figure 5). The sharp increase in the rate of tissue browning in the stem section compared with the other structures in the bud could be the result of the surpassing of the supercooling capacity of the pith parenchyma cells, as seen in blueberry (Kishimoto et al. 2014).

In the case of the bud axis, SAM and flower primordia, the observed tissue browning may be the result of gradual dehydrative stress, due to the water migration to the ice sink force from the bud scales. This stress causes injuries in cell membrane components subsequently seen as tissue browning (Steponkus 1984, Pearce 2001). It is not clear how levels of tissue browning in individual bud structures relate to the spectrum of injury, leading to damage. The lowest levels may result in impairment of tissue functionality that may not necessarily correspond to lethal damage. A pairing of CFT and regrowth assays, such as the ones performed by Workmaster and Palta (2006) in spring, could help to identify correlations between severity of damage to bud structures and development of new growth in fall samples; however, the obstacle of endodormancy in the bud's ability to grow at this time would be a major limitation.

Conclusions

From the results of our study, we consider the lack of detectable LTEs, the formation of voids in bud scale mesophyll, the freezing behavior of bud regions observed by the MRI scans, the different levels of INA for the bud structures, the progressive nature of CFT bud tissue damage and the differential expression of CFT damage across bud structures as collective evidence that cranberry terminal buds survive freezing stress through freeze-induced dehydration, as opposed to deep supercooling. These methods of evaluation are useful as phenotyping tools for the selection of plant material with improved freezing stress tolerance.

Supplementary Data

Supplementary Data are available at *Tree Physiology* online

Acknowledgments

We would like to thank Nicole Hansen from Cranberry Creek, Inc., and Bill Wolfe from Wisconsin River Cranberry Co. for supporting our research by allowing access to their farms. We would like to thank Beth Rauch of the Department of Medical Physics for access to the MRI facility and for operating the instrument during scanning runs. Also, thanks to Michael Wisniewski for assisting with the microthermocouple testing and to Jiwan Palta for access to the circulating glycol bath, as well as a thorough review of the manuscript and valuable suggestions. Finally, thanks to the undergraduate students collaborating with this research: Erin

Foley, Andi Nelson, Sarah Smilanich, Veronica Uribe and Lillian Zander.

Authors' contributions

Study conception and design was carried out by A.A., B.A.W. and C.V. Methodology implementation was by A.A., B.A.W., C.V. and J.B.-M. Experiment execution was performed by C.V. and S.S. Data collection was carried out C.V. and S.S. Data analysis/interpretation was performed by A.A., B.A.W., C.V. and J.B.-M. Manuscript writing/revision was done by A.A., B.A.W. and C.V.

Funding

This research is based upon work supported by the National Institute of Food and Agriculture, US Department of Agriculture, through a Hatch project 1009297 by the College of Agricultural and Life Sciences, University of Wisconsin–Madison and by the Wisconsin Cranberry Research and Education Foundation.

References

Abdallah AY, Palta JP (1989) Changes in the freezing stress resistance of the cranberry leaf, flower bud, and fruit during growth and development. Acta Hortic 241:273–276.

Andrews PK, Proebsting EL Jr (1986) Development of deep supercooling in acclimating sweet cherry and peach flower buds. Hortscience 21:99–100.

Ashworth EN (1990) The formation and distribution of ice within forsythia flower buds. Plant Physiol 92:718–725.

Bolivar-Medina JL, Zalapa J, Atucha A, Patterson SE (2018) Relationship of alternate bearing and apical bud development in cranberry (*Vaccinium macrocarpon* Ait.). Botany 97:101–111.

Danyluk J, Perron A, Houde M, Limin A, Fowler B, Benhamou N, Sarhan F (1998) Accumulation of an acidic dehydrin in the vicinity of the plasma membrane during cold acclimation of wheat. Plant Cell 10:623–638.

DeMoranville C, Demoranville I (1997) Cold tolerance of cranberry flower buds differs by cultivar and developmental stage. Hortscience 32:538A.

Eaton GW, Mahrt BJ (1977) Cold hardiness testing of cranberry flower buds. Can J Plant Sci 57:461–465.

Einhorn TC, Turner J, Gibeaut D, Postman JD (2011) Characterization of cold hardiness in quince: potential pear rootstock candidates for northern pear production regions. Acta Hortic 909:137–143.

Endoh K, Kuwabara C, Arakawa K, Fujikawa S (2014) Consideration of the reasons why dormant buds of trees have evolved extraorgan freezing as an adaptation for winter survival. Environ Exp Bot 106:52–59.

Flinn CL, Ashworth EN (1994*a*) Blueberry flower-bud hardiness is not estimated by differential thermal analysis. J Am Soc Hort Sci 119:295–298.

Flinn CL, Ashworth EN (1994*b*) Seasonal changes in ice distribution and xylem development in blueberry flower buds. J Am Soc Hort Sci 119:1176–1184.

George MF, Burke MJ, Pellett HM, Johnson AG (1974*a*) Low temperature exotherm and woody plant distribution. Hortscience 9:519–522.

George MF, Burke MJ, Weiser CJ (1974*b*) Supercooling in overwintering azalea flower buds. Plant Physiol 54:29–35.

George MF, Becwar MR, Burke MJ (1982) Freezing avoidance by deep undercooling of tissue water in winter-hardy plants. Cryobiology 19:628–639.

Goldman M (1988) Quantum description of high-resolution NMR in liquids. Oxford University Press, New York.

Gu L, Hanson PJ, Post WM, Kaiser DP, Yang B, Nemani R, Pallardy SG, Meyers T (2008) The 2007 eastern US spring freeze: increased cold damage in a warming world? Bioscience 58:253–262.

Ide H, Price WS, Arata Y, Ishikawa M (1998) Freezing behaviors in leaf buds of cold-hardy conifers visualized by NMR microscopy. Tree Physiol 18:451–458.

Ishikawa M (1982) Characteristics of freezing avoidance in comparison with freezing tolerance: a demonstration of extraorgan freezing. Academic Press, New York, NY. pp 325–340.

Ishikawa M, Sakai A (1981) Freezing avoidance mechanisms by supercooling in some rhododendron flower buds with reference to water relations. Plant Cell Physiol 22:953–967.

Ishikawa M, Sakai A (1985) Extraorgan freezing in wintering flower buds of *Cornus officinalis* Sieb. Et Zucc. Plant Cell Environ 8:333–338.

Ishikawa M, Price WS, Ide H, Arata Y (1997) Visualization of freezing behaviors in leaf and flower buds of full-moon maple by nuclear magnetic resonance microscopy. Plant Physiol 115:1515–1524.

Ishikawa M, Ishikawa M, Toyomasu T, Aoki T, Price WS (2015) Ice nucleation activity in various tissues of rhododendron flower buds: their relevance to extraorgan freezing. Front Plant Sci 25;6:149.

Kang SK, Motosugi H, Yonemori K, Sugiura A (1998) Supercooling characteristics of some deciduous fruit trees as related to water movement within the bud. J Hortic Sci Biotechs 73:165–172.

Kishimoto T, Sekozawa Y, Yamazaki H, Murakawa H, Kuchitsu K, Ishikawa M (2014) Seasonal changes in ice nucleation activity in blueberry stems and effects of cold treatments in vitro. Environ Exp Bot 106:13–23.

Koster KL, Lynch DV (1992) Solute accumulation and compartmentation during the cold acclimation of puma rye. Plant Physiol 98:108–113.

Kuprian E, Munkler C, Resnyak A, Zimmermann S, Tuong TD, Gierlinger N, Müller T, Livingston DP, Neuner G (2017) Complex bud architecture and cell-specific chemical patterns enable supercooling of Picea abies bud primordia. Plant Cell Environ 40:3101–3112..

Larsen HJ (2009) Evaluating tree fruit bud & fruit damage from cold. Colorado State University Extension. https://extension.colostate.edu/topic-areas/yard-garden/evaluating-tree-fruit-bud-fruit-damage-from-cold-7-426/ (10 October 2018, date last accessed).

Levitt J (1980) Responses of plants to environmental stress. In: Kozlowski TT (ed) Chilling, freezing, and high temperature stresses, Vol. 1, 2nd edn. Academic Press, London, New York.

McCown BH, Zeldin EL (2003) 'HyRed', an early, high fruit color cranberry hybrid. HortScience 38: 304–305.

Mills LJ, Ferguson JC, Keller M (2006) Cold-hardiness evaluation of grapevine buds and cane tissues. Am J Enol Viticult 57:194–200.

NOAA, MRCC (2019) 'cli-MATE'. https://mrcc.illinois.edu/CLIMATE/ (accessed 9 January 2019).

Olszewski F, Jeranyama P, Kennedy CD, DeMoranville CJ (2017) Automated cycled sprinkler irrigation for spring frost protection of cranberries. Agric Water Manag 189:19–26.

Pearce RS (2001) Plant freezing and damage. Ann Bot 87:417–424.

Price WS, Ide H, Arata Y, Ishikawa M (1997*b*) Visualization of freezing behaviors in flower bud tissues of cold-hardy Rhododendron japonicum by nuclear magnetic resonance micro-imaging. Funct Plant Biol 24:599–605.

Price WS, Ide H, Ishikawa M, Arata Y (1997*a*) Intensity changes in ^{1}H-NMR micro-images of plant materials exposed to subfreezing temperatures. Bioimages 5:91–99.

Quamme HA (1974) An exothermic process involved in the freezing injury to flower buds of several Prunus species. J Am Soc Hort Sci 99:315–318.

Quamme HA (1978) Mechanism of supercooling in overwintering peach flower buds. J Am Soc Hort Sci 103:57–61.

Quamme HA (1995) Deep supercooling in buds of woody plants. In: Lee RE, G JW, Gusta LV (eds) Biological ice nucleation and its applications. APS Press, Minneapolis, MN, pp 183–199.

Quamme HA, Su WA, Veto LJ (1995) Anatomical features facilitating supercooling of the flower within the dormant peach flower bud. J Am Soc Hort Sci 120:814–822.

Roper TR, Planer TD (1993) Cranberry production in Wisconsin. Wisconsin Cranberry Board, Wisconsin Rapids, p 6.

Sakai A (1979) Deep supercooling of winter flower buds of *Cornus florida* L. Hortscience 14:69–70.

Sakai A (1982) Freezing tolerance of shoot and flower primordia of coniferous buds by extraorgan freezing. Plant Cell Physiol 23:1219–1227.

Schneider CA, Rasband WS, Eliceiri KW (2012) NIH image to ImageJ: 25 years of image analysis. Nat Methods 9:671.

Snyder RL, de Melo-Abreu JP (2005) Frost protection: fundamentals, practice and economics. Food and Agriculture Organization of the United Nations, Rome.

Steffen KL, Arora R, Palta JP (1989) Relative sensitivity of photosynthesis and respiration to freeze-thaw stress in herbaceous species: importance of realistic freeze-thaw protocols. Plant Physiol 89:1372–1379.

Steponkus PL (1984) Role of the plasma membrane in freezing injury and cold acclimation. Annu Rev Plant Physiol 35: 543–584.

Vasseur DA, DeLong JP, Gilbert B, Greig HS, Harley CDG, McCann KS, Savage V, Tunney TD, O'Connor MI (2014) Increased temperature variation poses a greater risk to species than climate warming. Proc Biol Sci 281:20132612.

Wanner LA, Junttila O (1999) Cold-induced freezing tolerance in Arabidopsis. Plant Physiol 120:391–400.

Welin BV, Olson Å, Nylander M, Palva ET (1994) Characterization and differential expression of dhn/lea/Rab-like genes during cold acclimation and drought stress in *Arabidopsis thaliana*. Plant Mol Biol 26:131–144.

Williams CM, Henry HAL, Sinclair BJ (2015) Cold truths: how winter drives responses of terrestrial organisms to climate change. Biol Rev 90:214–235.

Wisniewski M (1995) Deep supercooling in woody plants and the role of cell wall structure. In: Lee RE, G JW, Gusta LV (eds) Biological ice nucleation and its applications. APS Press, Minneapolis, MN, pp 163–181.

Wisniewski M, Lightner G, Davis G, Schiavone M (1990) System configuration for microcomputer-controlled, low-temperature differential thermal analysis. Comput Electron Agr 5:223–232.

Wisniewski M, Gusta L, Neuner G (2014) Adaptive mechanisms of freeze avoidance in plants: a brief update. Environ Exp Bot 99:133–140.

Workmaster BAA, Palta JP (2006) Shifts in bud and leaf hardiness during spring growth and development of the cranberry upright: regrowth potential as an indicator of hardiness. J Am Soc Hort Sci 131:327–337.